

Yanyan Wang

School of Engineering and Technology,
China University of Geosciences (Beijing),
Beijing 100083, China
e-mail: wangyy6711@163.com

Yang Wang

School of Engineering and Technology,
China University of Geosciences (Beijing),
Beijing 100083, China
e-mail: 545714553@qq.com

Jiajie Kang¹

School of Engineering and Technology,
China University of Geosciences (Beijing),
Beijing 100083, China;
State Key Laboratory of Tribology,
Department of Mechanical Engineering,
Tsinghua University,
Beijing 100084, China;
Zhengzhou Research Institute,
China University of Geosciences (Beijing),
Zhengzhou 451283, China
e-mail: kangjiajie@cugb.edu.cn

Guozheng Ma¹

National Key Lab for Remanufacturing,
Academy of Armored Forces Engineering,
Beijing 100072, China
e-mail: magz0929@163.com

Lina Zhu

School of Engineering and Technology,
China University of Geosciences (Beijing),
Beijing 100083, China;
Zhengzhou Research Institute,
China University of Geosciences (Beijing),
Zhengzhou 451283, China
e-mail: zhulina@cugb.edu.cn

Haidou Wang

School of Engineering and Technology,
China University of Geosciences (Beijing),
Beijing 100083, China;
National Key Lab for Remanufacturing,
Academy of Armored Forces Engineering,
Beijing 100072, China
e-mail: wanghaidou@aliyun.com

Zhiqiang Fu

School of Engineering and Technology,
China University of Geosciences (Beijing),
Beijing 100083, China;
Zhengzhou Research Institute,
China University of Geosciences (Beijing),
Zhengzhou 451283, China
e-mail: fuzq@cugb.edu.cn

Tribological Properties of Ti-Doped Diamond-Like Carbon Coatings Under Boundary Lubrication With ZDDP

Diamond-like carbon (DLC) coatings containing 0.7%, 5.8%, and 23.3% Ti were deposited via pulsed cathodic arc deposition and magnetron sputtering on AISI 316L stainless steel substrates. The varied Ti content was controlled by setting Ti target current at 3, 5, and 7A. The composition, microstructure, mechanical, and tribological properties of Ti-doped DLC (Ti-DLC) coatings were investigated using X-ray photoelectron spectroscopy, Raman spectroscopy, nanoindentation, and ball-on-disc tribometer. The results show that TiC formed when Ti content in the coating was higher than 5.8 at% and the I_D/I_G ratios increased gradually with the increasing Ti content. Ti-DLC with 0.7 at% Ti had the highest H/E and H^3/E^2 ratios and exhibited optimal tribological properties under lubrication, especially when zinc dialkyldithio-phosphate (ZDDP) was contained in the oil. Furthermore, ZDDP tribofilms played an important role in wear reduction by protecting the rubbing surfaces against the adhesion and suppressing the tribo-induced graphitization of DLC coatings. [DOI: 10.1115/1.4049373]

Keywords: Ti-DLC, mechanical properties, tribological properties, lubrication, ZDDP

¹Corresponding author.

Contributed by the Tribology Division of ASME for publication in the JOURNAL OF TRIBOLOGY. Manuscript received March 11, 2020; final manuscript received September 22, 2020; published online January 13, 2021. Assoc. Editor: Wenyang Zhang.

Haipeng Huang

Beijing Research Institute,
Sinopec Lubricant Co., Ltd.,
Beijing 100085, China
e-mail: huanghp.lube@sinopec.com

Wen Yue

School of Engineering and Technology,
China University of Geosciences (Beijing),
Beijing 100083, China;
Zhengzhou Research Institute,
China University of Geosciences (Beijing),
Zhengzhou 451283, China
e-mail: cugbyw@163.com

Introduction

Diamond-like carbon (DLC) coatings with mixed structures of sp^2 - and sp^3 -bonded carbon atoms possess the advantages of good friction and wear resistance, high hardness, and chemical inertness [1]. Since first prepared by ion beam deposition (IBD) in 1971, DLC coatings have been one of the most valuable and promising types of protective coatings applied in the mechanical field [1–4]. For instance, they are potentially applied to automotive valve train components, e.g., cams, tappets, and pistons [3]. In decades years, researchers have tried to prepared DLC coatings by chemical vapor deposition (CVD) and physical vapor deposition (PVD), e.g., plasma-enhanced CVD (PECVD), plasma-assisted CVD (PACVD), IBD, filtered cathodic vacuum arc (FCVA), pulsed cathodic arc deposition (PCAD), and magnetron sputtering (MS) [5,6].

Nevertheless, it has been demonstrated that DLC coatings exhibit higher residual stress, low toughness, and poor adhesion to the substrate. Doping metal elements (Ti, W, Cr, Ag) into them is an effective way to overcome these obstacles [7–11]. Ti is a widely studied doping metal due to its good adhesion to most substrates. Furthermore, Ti can react with carbon to form TiC nanocrystallites embedded in DLC matrixes, which enhances the wear resistance and oxidation resistance of the DLC coating in some conditions [12,13]. Recently, many researchers have focused on the mechanical and tribological properties of Ti-doped DLC (Ti-DLC) coatings [6,12,14–24] and their studies are summarized in Table 1. The results show that Ti content doping into the DLC coatings was as

high as 30 at% and it made a significant influence on the microstructure, mechanical, and tribological properties of the DLC coatings.

Most mechanical components work under boundary or mixed lubrication and their tribological properties depend on the surface properties of component material and the properties of commercial lubricants containing various types of additives. Thus, understanding the interactions between DLC coatings and additives is referable for lubricant manufacturers to produce lubricants able to be effective with many types of DLC coatings [25]. Many researchers have studied the tribological properties of non-doped or metal-doped DLC coatings lubricated with the base oil, lubricant additives, and fully formulated oil [25–29], and the results varied with the types of coating and lubricant. In general, zinc dialkyldithiophosphate (ZDDP), the most widely used antiwear additive, can chemically decompose and form tribofilms on DLC coatings, but the tribofilms are thinner and with lower tenacity comparing to those formed on metal surfaces [30]. For Ti-DLC coatings, a little work has been done on their friction and wear behaviors under oil lubrication. Kalin et al. [31] confirmed the high reactivity of Ti-DLC coating by static reactivity experiments, leading to low wear rate under dialkyl dithiophosphate additive contained lubrication. de Barros’Bouchet et al. [10] reported that Ti-DLC coatings had less friction and wear loss than non-doped DLC coating under the base oil lubrication regardless of the counterparts (the same coating or steel). But there were minor differences between them when molybdenum dithiocarbamate (MoDTC) and ZDDP were contained in the base oil. The recent report by Guo et al.

Table 1 A review of deposition methods and mechanical and tribological properties of Ti-DLC coatings

Deposition method	Ti content (at%)	Substrate	Hardness (GPa)	Elastic modulus (GPa)	Tribotest condition	Friction coefficient
MS [13]	0.82–1.97	17-4 steel	11.9–44.6	154.1–368.2	Dry sliding	0.008–0.02
PACVD + MS [14]	5	100Cr6	12	120	Base oil (BO) BO + AW ^a /EP ^b additive BO + EP additive	0.3–0.4
MS [15]	0.41–8.2	Si wafer	10–14	110–120	Dry sliding	0.05–0.14
CVD + MS [16]	5.3	Ti6Al4V alloy	24.5		Dry sliding	–
IBD + MS [17]	3.78–23.57	Si wafer	~28	~247.7	Dry sliding	0.13–0.25
MS [18]	~22	316L SS	15–20	200–230	Water lubrication	0.081–0.148
MS [19]	0.3	Si wafer	9	90	Dry sliding	0.036
MS [20]	0.4–3.77	316L SS	2–2.5	49.1–95.6	Dry sliding	0.33–0.61
MS [21]	1.2–5.8	304 SS	15.2–16.7	128.6–138.5	Dry sliding Water lubrication	0.09–0.18 0.08–0.11
PCAD + MS [22]	1.4–9.75	Si wafer	11.1–11.9		Dry sliding	0.17–0.21
IBD + MS [23]	4, 27	Si wafer	16.8, 23.6	158.3, 221.5	Dry sliding PAO lubrication	0.07–0.30 0.09–0.13
MS [24]	0.2–1.6	304 SS	14.8–21.6	170–185	Dry sliding	0.13–1.16

^aAW: antiwear.

^bEP: extreme pressure.

Table 2 Tribotest condition

Parameter	Test condition
Oil	PAO4 and PAO4+ZDDP
Temperature	100 °C
Load/contact pressure	7 N/0.7–0.9 GPa
Reciprocating amplitude	4 mm
Reciprocating frequency	5 Hz
Test duration	1800 s

[23] compared the tribological properties of Ti-DLC coatings with 4% and 27% Ti under dry sliding and oil lubrication. It revealed that Ti-DLC coating with low Ti content exhibited better tribological performances than that with high Ti content under both dry and oil lubrication conditions. However, the interactions between additives and DLC coatings are governed by various factors (temperature, contact pressure, properties of contact surfaces, etc.), which is quite complex. Fundamental research is necessary to reveal the effect of microstructure on the interactions between Ti-DLC coatings and additives, since it is rarely reported.

In this work, Ti-DLC coatings with various Ti contents were deposited on AISI 316L stainless steel substrate, and the relationships between composition, microstructure, and mechanical properties were investigated. ZDDP was selected as the experimental additive, which is an irreplaceable antiwear additive in the mechanical industry owing to its good oxidation resistance and ability to form tribofilm on the contacting surfaces [32]. The friction and wear behaviors of Ti-DLC coatings under base oil and ZDDP-contained lubrications were investigated.

Experimental Details

Coating Deposition. Ti-DLC coatings (2.3 μm thick, $R_a = 0.02\text{--}0.04 \mu\text{m}$) were deposited on AISI 316L stainless steel substrate (size of 60 mm \times 60 mm \times 3 mm, $R_a = 0.004 \mu\text{m}$) by the PCAD+MS method. First, the substrates were ultrasonically

cleaned in acetone and dried in the air, and then etched by Ar gas (purity 99.99%) for 10 min in the chamber at the pressure of 0.5 Pa to remove the absorbed contaminations. Then, a thin Ti interlayer was deposited on the steel substrate to enhance the coherent strength. Finally, Ti-DLC coatings were deposited in C_2H_2 (purity 99.99%) and Ar atmosphere sputtering with two rectangular Ti targets (purity 99.99%) as the metal source. By setting the Ti target currents at 3, 5, and 7 A, Ti-DLC coatings with 0.7 at%, 5.8 at%, and 23.3 at% Ti were obtained, named as $\text{Ti}_{0.7}\text{-DLC}$, $\text{Ti}_{5.8}\text{-DLC}$, and $\text{Ti}_{23.3}\text{-DLC}$, respectively. Pure DLC coating, i.e., non-doped coating, was also prepared using a pure graphite target for comparison. Then, the coated steel plates were cut into small pieces and cleaned by acetone in an ultrasonic bath for 15 min followed by the analysis.

Tribotests. Tribological properties of the pure DLC and Ti-DLC coatings under lubrication conditions were investigated using a ball-on-disc tribometer (CSM-TRN). The base oil was synthetic poly-alpha-olefin of viscosity grade 4 (PAO4) and ZDDP (10.0% Zn, 8.0% P, and 16.0% S) was added into PAO4 with a concentration of 1 wt%. AISI 52100 steel ball with a diameter of 6 mm, the hardness of 770 HV, and R_a of 0.025 μm was used as the counterpart sliding on the coated disc. For each test, 2 ml oil was introduced to the counterbodies at room temperature, and then, the test started when the temperature rose to the setpoint (100 °C) within 10 min. More detailed parameters are listed in Table 2. For each type of oil and coating, three different tests with identical conditions were performed to ensure the reproducibility of the friction behaviors.

The calculated lambda (λ) value, equals to the ratio of calculated minimum oil film thickness (h_{min}) to composited surface roughness [33], was 0.08–0.1. It reveals that the friction and wear occurred under the boundary lubrication regime. After the tribotests, the coated discs were ultrasonically cleaned in acetone for 15 min to remove residual oil.

Surface Characterization. A scanning electron microscopy (SEM, Siricon 200) was used to investigate the surface

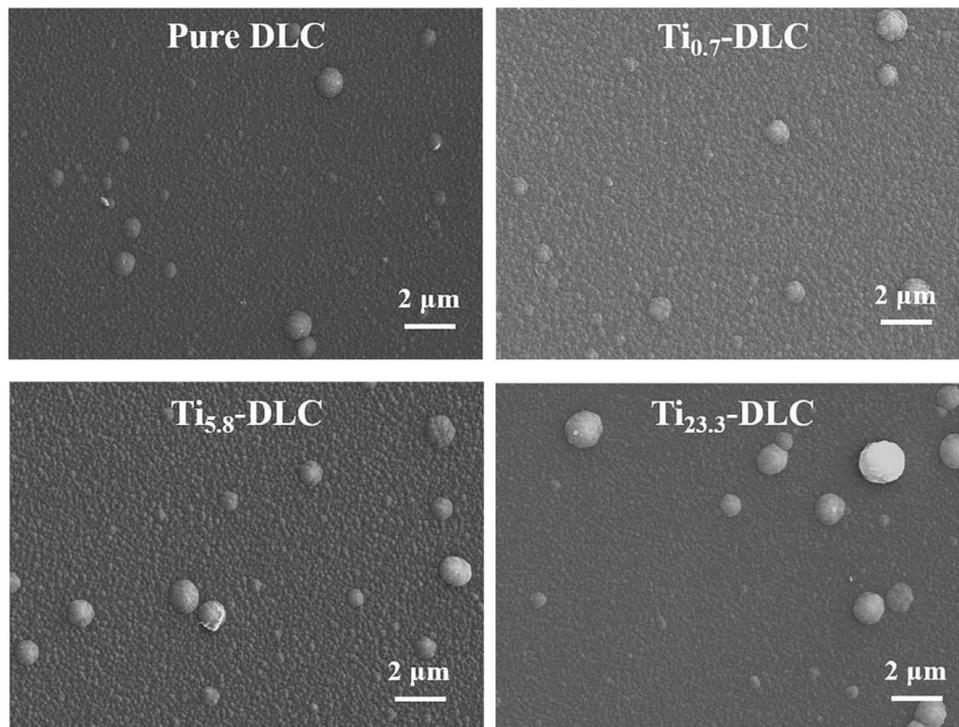


Fig. 1 Scanning electron microscopy morphology images of DLC coatings

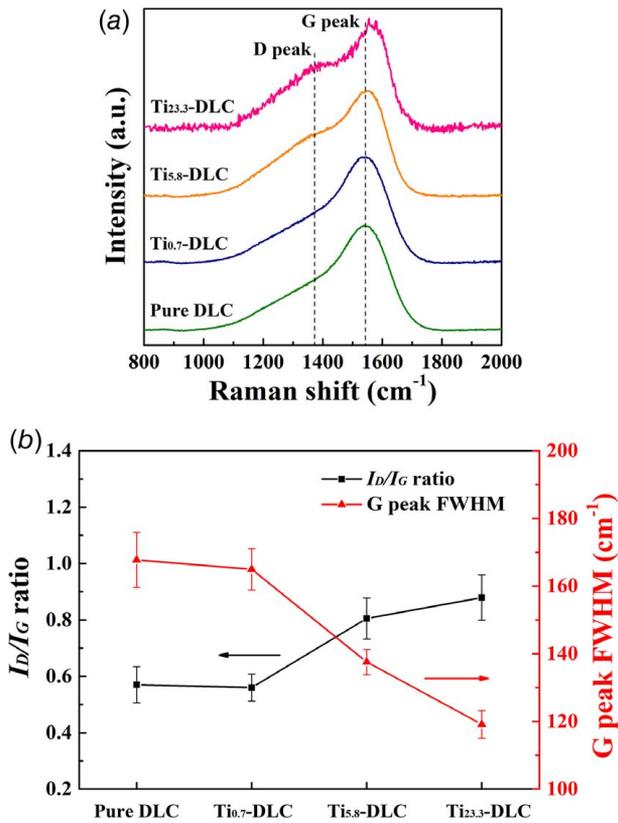


Fig. 2 (a) Raman spectra and (b) I_D/I_G ratios and G peak FWHM of the DLC coatings

morphologies of DLC coatings. The hardness and elastic modulus were measured using a nanoindentation (CSM UNHT) with a standard diamond Berkovich tip. The indentation tests were conducted at three to five positions on each sample in a continuous stiffness measurement mode and the maximum penetration was 10% of the coating thickness to avoid the influence of the substrate. Raman spectra were used to evaluate the carbon atomic bond structures of DLC coatings, being obtained by a Raman spectroscopy (Renshaw 2000) with a 514.5 nm laser. The data were taken at three to five spots on each sample with 20 s exposure time. The deconvolution of the peaks was executed by curve fitting using the Gaussian-Lorentz function. Chemical compositions of DLC coatings and tribofilms were detected using an X-ray photoelectron spectroscopy (XPS; PHI Quantera SXM) with an Al $K\alpha$ X-ray source. The tested surfaces were sputtered for 3 nm in depth by Ar⁺ to remove the adsorbed contaminant. The binding energy was calibrated with C 1s = 284.8 eV.

Wear rates of pure DLC and Ti-DLC coatings were calculated using Archard wear equation: $k = V/FS$, where V is the wear volume (m³), F is the normal load (N), and S is the sliding distance (m). Wear scars on the steel balls were observed using an optical microscope (BX51M Olympus). A surface profilometer (NanoMap-D) with optical mode was used to measure the roughness and wear volumes by scanning the surfaces and wear tracks of coatings, respectively.

Results and Discussion

Microstructure, Composition, and Mechanical Properties. Surface morphologies of pure DLC and Ti-DLC coatings investigated using SEM are shown in Fig. 1. It was observed that some particles existed on all coating surfaces, which were caused by the droplet splashing of the cathode arc during the preparation of

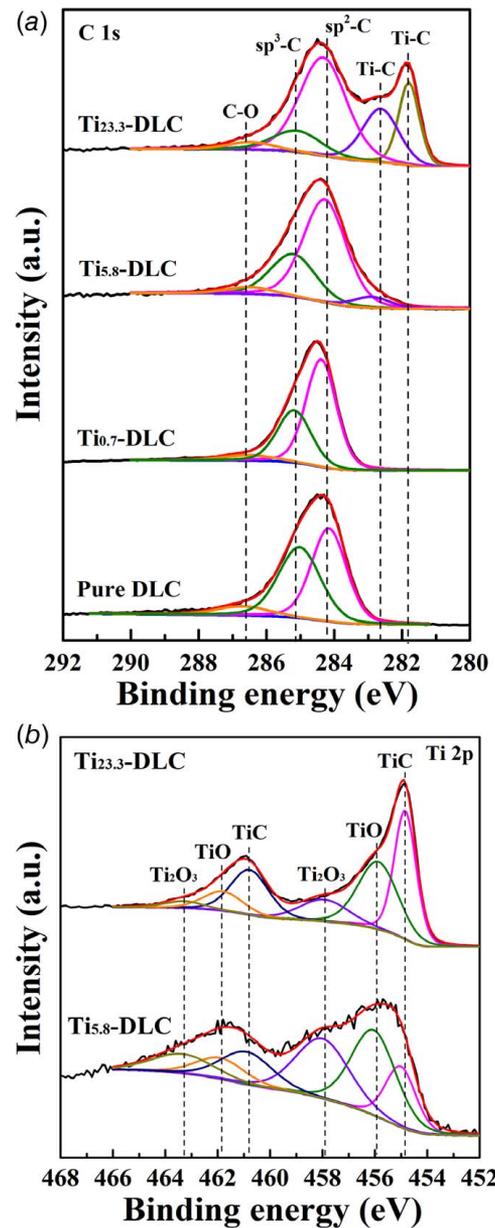


Fig. 3 (a) C 1s and (b) Ti 2p spectra of the DLC coatings

the interlayer. This means doping Ti element in this study had little influence on surface morphologies of DLC coatings.

Raman spectroscopy is regarded as an effective tool for the non-destructive characterization of the carbon bonding structure of the DLC coating. A typical Raman spectrum of DLC coating has two peaks, the so-called D peak and G peak. The intensity ratio of D peak to G peak (I_D/I_G) and the full-width at half maximum (FWHM) of G peak are used to evaluate the characteristics of DLC coating [34–36]. In Fig. 2(a), D peaks and G peaks in all

Table 3 Mechanical properties of the DLC coatings

Coating	Hardness (GPa)	Elasticity modulus (GPa)	H/E	H^3/E^2 (GPa)
Pure DLC	19.5 ± 1.24	156.3 ± 10.05	0.12	0.30
Ti _{0.7} -DLC	22.9 ± 2.16	194.8 ± 17.86	0.12	0.32
Ti _{5.8} -DLC	18.3 ± 1.40	151.6 ± 15.41	0.12	0.27
Ti _{23.3} -DLC	20.5 ± 1.47	269.8 ± 20.66	0.07	0.12

spectra are located at around 1380 cm^{-1} and 1560 cm^{-1} , respectively. Figure 2(b) shows that the I_D/I_G ratio increased from 0.56 to 0.88 and the G peak FWHM decreased from 167.7 cm^{-1} to 119.1 cm^{-1} as Ti content increased from 0 (pure DLC) to 23.3 at %. This indicates that $\text{sp}^2\text{-C}$ increased in the coating, due to the distortion of bond angles caused by Ti atoms and the formation of TiC [17,22].

Figure 3 shows the C 1s and Ti 2p XPS spectra of pure DLC and Ti-DLC coatings. C 1s peaks in Fig. 3(a) gave fit to $\text{sp}^2\text{-C}$, $\text{sp}^3\text{-C}$, and C-O at 284.3 ± 0.1 , 285.1 ± 0.1 , and $286.6 \pm 0.1\text{ eV}$, respectively. Furthermore, Ti-C peaks appeared at 281.8 ± 0.1 and $282.7 \pm 0.1\text{ eV}$ when Ti content was higher than 5.8 at%, revealing the presence of titanium carbide components [12,21,22]. Ti 2p

spectra in Fig. 3(b) further confirmed the existence of TiC in $\text{Ti}_{5.8}\text{-DLC}$ and $\text{Ti}_{23.3}\text{-DLC}$. However, the identification of the Ti phase for $\text{Ti}_{0.7}\text{-DLC}$ was difficult because of its low content and high spectral noise. Ti 2p spectra gave the best fit to six peaks at 454.9 ± 0.1 and $460.8 \pm 0.1\text{ eV}$, 455.9 ± 0.1 and $461.8 \pm 0.1\text{ eV}$, 457.9 ± 0.1 and $463.3 \pm 0.1\text{ eV}$ in $\text{Ti } 2p_{1/2}$ and $\text{Ti } 2p_{3/2}$, and they corresponded to TiC, TiO, and Ti_2O_3 , respectively [12,37–39]. According to the Ti dissolution limit in DLC coating (0.9–2.5 at %) reported by Meng et al. [40], doping Ti beyond the limit led to the precipitation of nanocrystalline TiC cluster in $\text{Ti}_{5.8}\text{-DLC}$ and $\text{Ti}_{23.3}\text{-DLC}$.

Table 3 lists the hardness (H), elasticity modulus (E), H/E , and H^3/E^2 ratios of the DLC coatings. The H/E and H^3/E^2 ratios are used to evaluate the plastic deformation resistance of hard nanocomposite coatings, which are positively correlated with wear resistance [41]. Compared to pure DLC, $\text{Ti}_{0.7}\text{-DLC}$ with low Ti content has higher hardness (22.9 GPa), due to the solid solution hardening effect by Ti doping [15,20]. For $\text{Ti}_{5.8}\text{-DLC}$ and $\text{Ti}_{23.3}\text{-DLC}$, it is the cooperation of increased $\text{sp}^2\text{-C}$ (soft phase) and TiC nanoparticles (hard phase) contributed to the small variance of their hardness (18.3 GPa and 20.5 GPa). Furthermore, the H/E and H^3/E^2 ratios varied with Ti content, and the general trends were similar to that of the hardness, which was the H/E and H^3/E^2 ratios of $\text{Ti}_{0.7}\text{-DLC}$ and $\text{Ti}_{23.3}\text{-DLC}$ were the highest and lowest, respectively.

Friction and Wear Behaviors. Figure 4 shows the friction coefficients of DLC coatings under PAO4 and PAO4+ZDDP lubrication conditions. It can be seen that the friction coefficients of all coatings reached a steady-state stage after a short running-in period (Figs. 4(a) and 4(b)), and the averaged steady coefficients were 0.119–0.134 under PAO4 lubrication and 0.115–0.129 under PAO4+ZDDP lubrication (Fig. 4(c)). For the PAO4 case, $\text{Ti}_{5.8}\text{-DLC}$ presented the highest friction coefficient, which was attributed to the hard TiC embedded in the DLC matrix [6,42]. However, the friction coefficient of $\text{Ti}_{23.3}\text{-DLC}$ dropped to the lowest and the curve fluctuated slightly. This may be attributed to the cooperation between the graphitization of the coating and the generation of abrasive particles. As shown in Fig. 4(c), the steady friction coefficient variation trend is different between PAO4 and PAO4+ZDDP lubrications. $\text{Ti}_{0.7}\text{-DLC}$ coating had a lower friction coefficient than others, which may be related to the interaction between the coatings and ZDDP. In addition, the friction coefficient of $\text{Ti}_{23.3}\text{-DLC}$ coating increased when ZDDP was introduced. It is possible that ZDDP molecules reduce the effectiveness of the low-friction surface of sp^2 -dominated Ti-DLC coating [25].

The wear rates of DLC coatings are shown in Fig. 5. On the one hand, the wear rates varied with Ti content, and the trend was opposite to that of H/E and H^3/E^2 ratios. $\text{Ti}_{0.7}\text{-DLC}$ with high H/E and

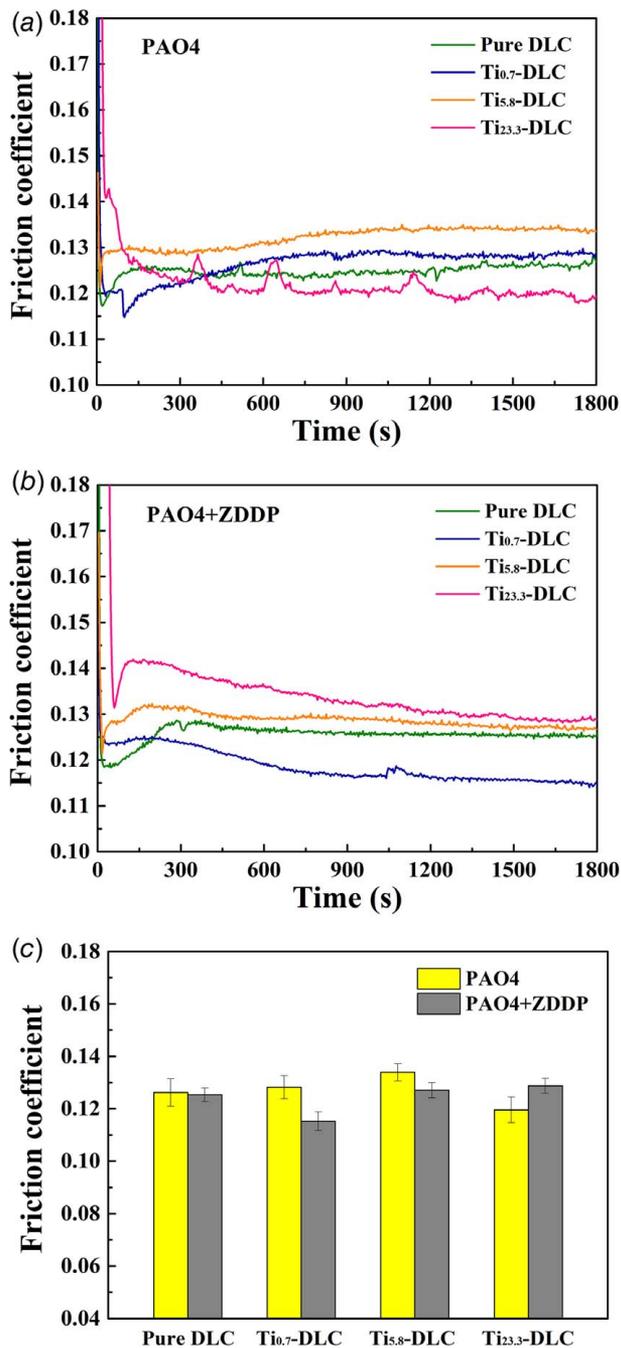


Fig. 4 Friction coefficients of the DLC coatings as a function of sliding time under (a) PAO4 and (b) PAO4+ZDDP lubrication conditions and (c) friction coefficients at steady-state stage (last 600 s)

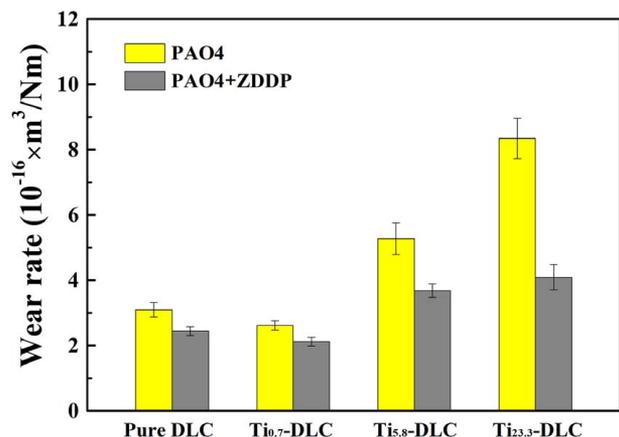


Fig. 5 Wear rates of the DLC coatings

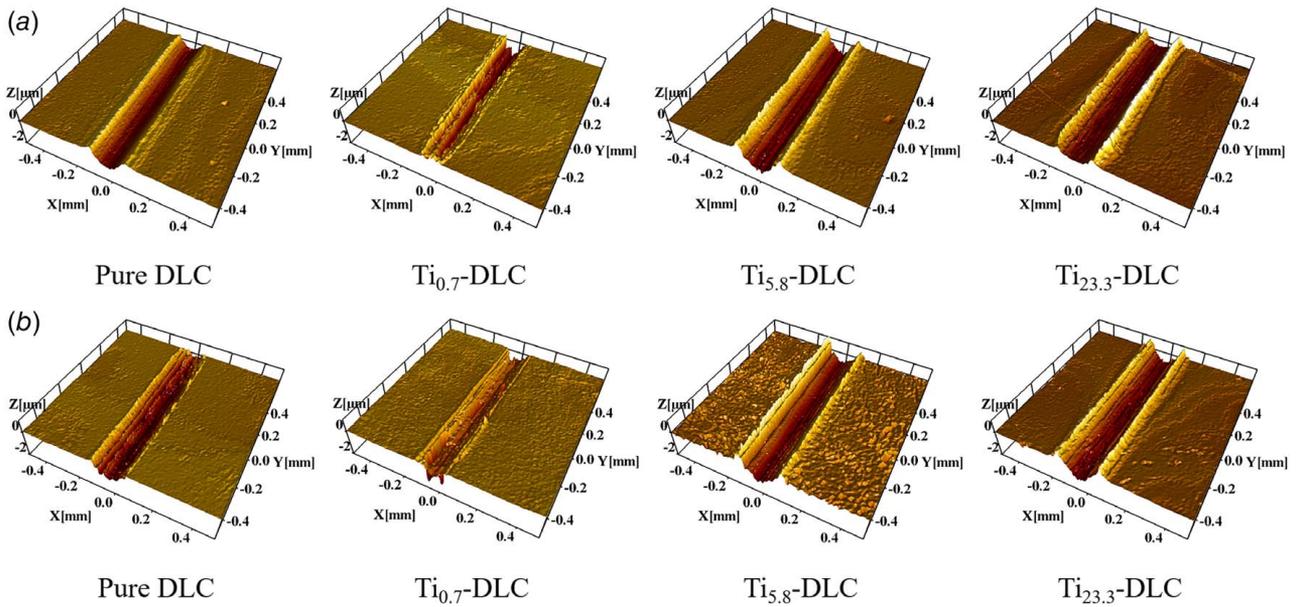


Fig. 6 Three-dimensional (3D) morphologies of wear tracks on DLC coatings under (a) PAO4 and (b) PAO4+ZDDP lubrication conditions

H^3/E^2 ratios had the ability to resist plastic deformation and presented better wear resistance than others. In addition, TiC and Ti oxides acting as abrasive particles aggravated the wear of $Ti_{5.8}$ -DLC and $Ti_{23.3}$ -DLC. The typical 3D morphologies of wear tracks in Fig. 6 indicate that abrasive wear occurred on all coatings and plastic deformation (material pileup at the two edges of the wear track) was severer for $Ti_{5.8}$ -DLC and $Ti_{23.3}$ -DLC. The furrows on $Ti_{0.7}$ -DLC were narrower and shallower than those on $Ti_{23.3}$ -DLC under two lubrications, leading to the difference in wear rates. On the other hand, compared to PAO4, ZDDP provided 21.1%, 19.1%, 30.2%, and 51.1% reduction in the wear rates for pure DLC, $Ti_{0.7}$ -DLC, $Ti_{5.8}$ -DLC, and $Ti_{23.3}$ -DLC, respectively. The reason maybe that graphitic carbon was easily removed during rubbing, but ZDDP decomposed to form tribofilm on the DLC

coatings and then prevented the rubbing surfaces from direct contact [8,25,43].

The morphologies of wear scars on steel balls were observed by means of optical microscopy as shown in Fig. 7. The balls against Ti-DLC coatings with high Ti content ($Ti_{5.8}$ -DLC and $Ti_{23.3}$ -DLC) suffered severer wear than those against the coatings with low Ti content (pure DLC and $Ti_{0.7}$ -DLC). Meanwhile, all wear scars were covered with colored layers, and the color was different under two lubrications.

Raman Analysis. Raman spectra of the worn DLC coatings and wear scars on steel ball are shown in Fig. 8. It is observed that the I_D/I_G ratios increased after wear (Fig. 2(b) and Figs. 8(a) and 8(b)),

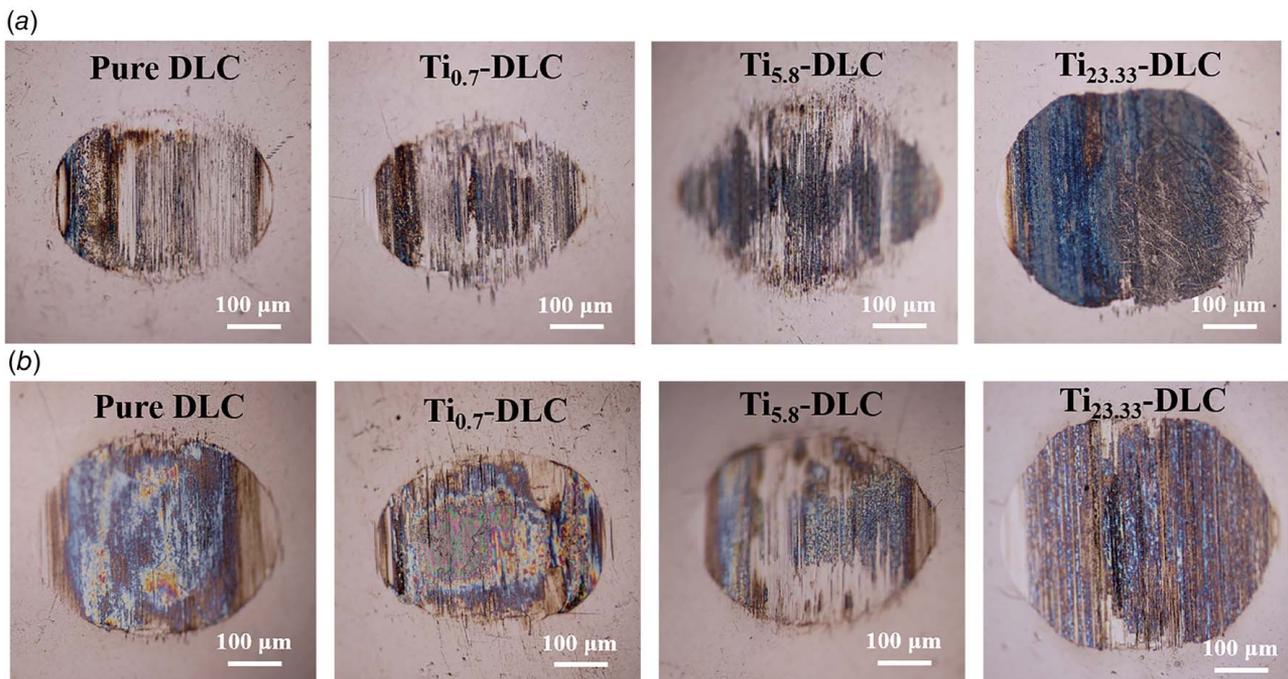


Fig. 7 Optical images of the wear scars on steel balls under (a) PAO4 and (b) PAO4+ZDDP lubrication conditions

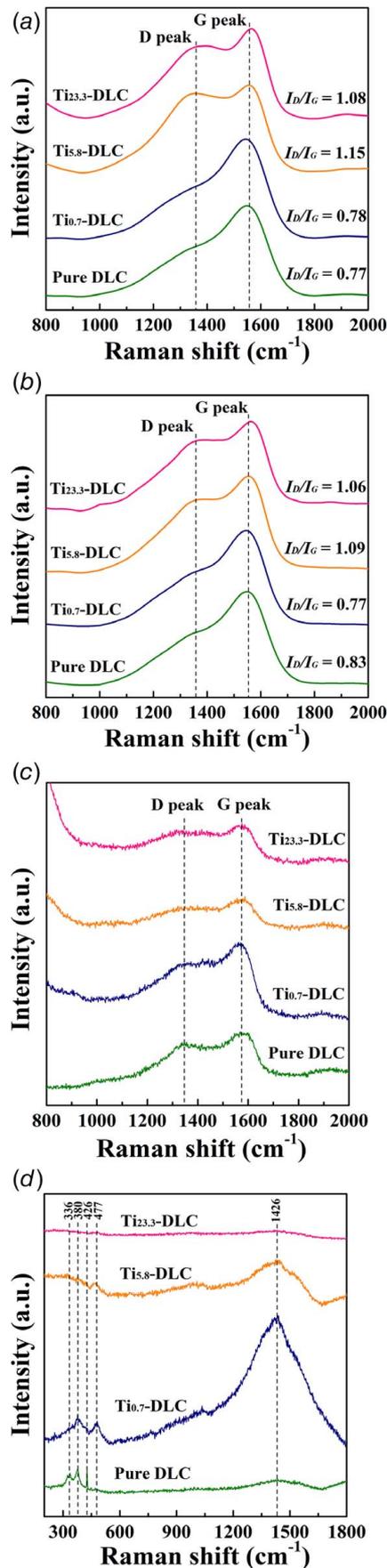


Fig. 8 Raman spectra of the worn DLC coatings and the wear scars on steel balls (a) DLC, PAO4; (b) DLC, PAO4+ZDDP; (c) ball, PAO4; and (d) ball, PAO4+ZDDP

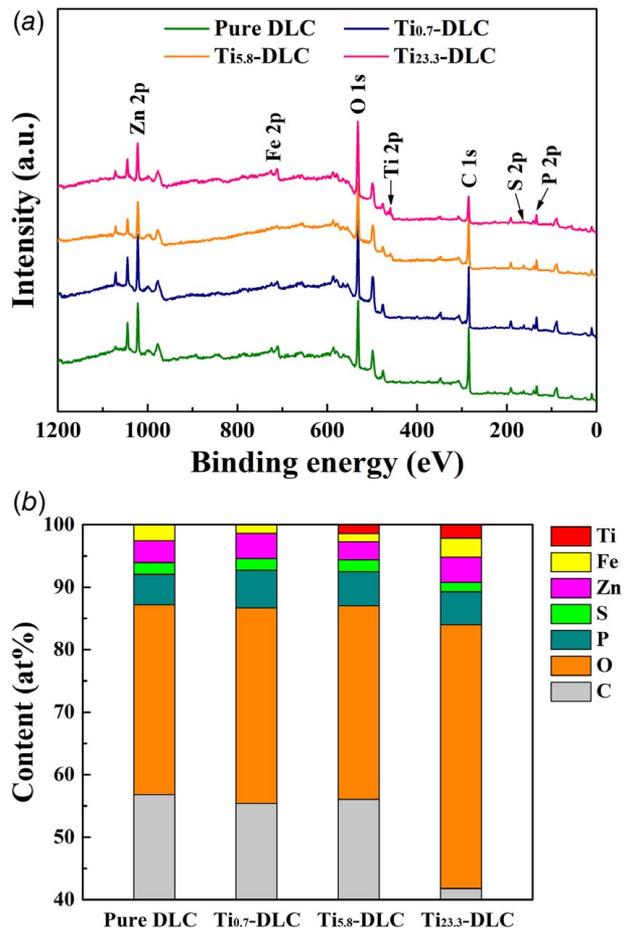


Fig. 9 (a) XPS survey spectra and (b) the element contents of the worn DLC coatings on ZDDP-contained occasion

due to the increased sp^2 -C content caused by frictional energy [24,44]. Moreover, the I_D/I_G ratios of the worn $Ti_{23.3}$ -DLC were lower than those of the worn $Ti_{5.8}$ -DLC under two lubrications, which was opposite to the variation trend before wear. This is because that the graphitic layer on $Ti_{23.3}$ -DLC was easily removed during rubbing and then led to the decrease in I_D/I_G ratio. The result is consistent with the wear rates in Fig. 5. Figure 8(c) shows that the peaks for steel ball under PAO4 lubrication were similar to those of original DLC coatings, which were D peak and G peak. Under PAO4+ZDDP lubrication (Fig. 8(d)), the peaks for steel ball at 336 and 380 cm^{-1} , 426 and 477 cm^{-1} were assigned to ZnS [45] and phosphate [46], respectively, and the peak at 1426 cm^{-1} belonged to the base oil [47]. This reveals that the covered layer was ZDDP tribofilm rather than the carbon layer. Therefore, the fact is that the carbon layer from DLC transferred onto the steel balls under PAO4 lubrication and ZDDP successfully protected the DLC/steel contacts against adhesion by forming tribofilm. The result is consistent with the literatures [48,49] report.

XPS analysis was carried out to reveal the chemical compositions of tribofilms. Figure 9(a) shows the survey spectra of the worn DLC coatings on ZDDP-contained occasion and the relative element contents were given in Fig. 9(b). It was observed that Fe coming from the steel ball and Zn, P, and S coming from ZDDP were detected on all coatings. Ti remained in the worn $Ti_{5.8}$ -DLC and $Ti_{23.3}$ -DLC, indicating the incompletable wear of the coatings.

Figure 10 shows the XPS detailed spectra of Zn 2p, P 2p, S 2p, and O 1s. Zn 2p spectra in Fig. 10(a) gave only one peak at 1022 ± 0.2 eV corresponding to ZnO/ZnS; P 2p spectra in Fig. 10(b) gave two peaks at 133.3 ± 0.1 and 134.2 ± 0.1 eV corresponding to

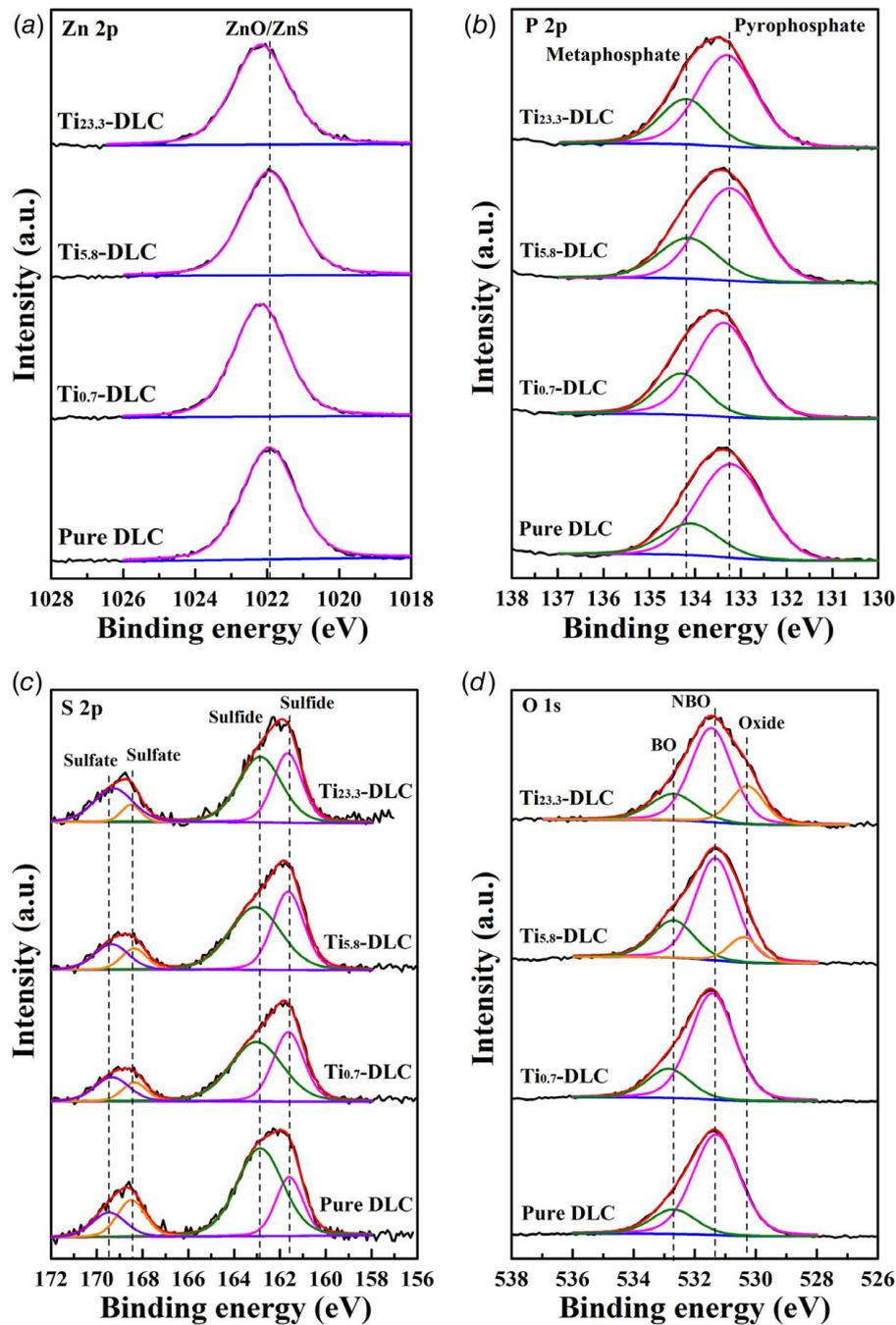


Fig. 10 XPS detailed spectra of (a) Zn 2p, (b) P 2p, (c) S 2p, and (d) O 1s obtained from ZDDP tribofilms on the worn DLC coatings

pyrophosphate and metaphosphate, respectively [49,50]; S 2p spectra in Fig. 10(c) gave four peaks at 161.7 ± 0.1 and 163 ± 0.1 eV corresponding to metal sulfides, 168.5 ± 0.1 and 169.4 ± 0.1 eV corresponding to metal sulfates [30,38,50]. It was reported that metal sulfate was the initial decomposition product of ZDDP which indicated its incompletable decomposition during the 30 min rubbing [30]. The peaks for O 1s at 530.4 ± 0.1 , 531.4 ± 0.1 , and 532.7 ± 0.1 eV were assigned to the metal oxides, non-bridging oxygen (P=O and P-O-M), and bridging oxygen (P-O-P), respectively (Fig. 10(d)) [49,50].

BO/NBO ratio is a usually used parameter to identify the chain length of polyphosphate [50,51]. The calculated BO/NBO ratios listed in Table 4 were 0.23, 0.25, 0.38, and 0.33 for the worn pure DLC, Ti_{0.7}-DLC, Ti_{5.8}-DLC, and Ti_{23.3}-DLC, respectively. It

reveals that the polyphosphate chain length for all coatings was intermediate between pyrophosphate and metaphosphate [51,52]. This is also confirmed by P 2p spectra in Fig. 10(b).

According to the analyses in this study, the main govern factor for friction and wear behaviors of Ti-DLC coatings is Ti content. It affects the mechanical properties by leading to graphitization

Table 4 BO/NBO ratios of the worn DLC coatings

Coating	Pure DLC	Ti _{0.7} -DLC	Ti _{5.8} -DLC	Ti _{23.3} -DLC
BO/NBO ratio	0.23	0.25	0.38	0.30

and generation of TiC when Ti content was higher 5.8 at%. As a hard phase, TiC can aggravate the abrasive wear of Ti_{5.8}-DLC and Ti_{23.3}-DLC under PAO4 lubrication, especially when graphitization occurred on the coating during rubbing. Therefore, Ti_{23.3}-DLC presented the lowest friction coefficient but the highest wear rate under PAO4 lubrication. Furthermore, ZDDP can prevent the counterbodies from direct contact and suppress wear by decomposing to form tribofilms composed of phosphate and sulfides/sulfates. As a consequence, the wear rates of all coatings under PAO4+ZDDP lubrication were lower than those under PAO4 lubrication. In addition, Ti content in DLC coating will affect the effort of ZDDP tribofilm, which means higher hardness and less abrasive particles for Ti-DLC with low Ti content may facilitate the formation and maintaining of tribofilm.

Conclusions

Ti-DLC coatings with 0.7–23.3 at% Ti were deposited on AISI 316L stainless steel substrates. The composition analysis reveals that the dissolution limit of the doped Ti atoms was less than 5.8 at%. When doping Ti less than its dissolution limit, the Ti-DLC coatings had a similar structure with the pure DLC coating. However, as the Ti content rose beyond the limit value, graphitic carbon (sp²-C) increased and TiC and Ti oxides nanoparticles formed in the coatings. As a consequence, the mechanical properties varied with Ti content. Under PAO4 lubrication, the friction and wear behaviors of DLC coatings were mainly governed by the H/E and H^3/E^2 ratios and a carbon layer transferred onto the steel ball during rubbing. However, the tribofilms mainly consisting of polyphosphates and sulfides/sulfates played an important role in wear reduction under PAO4+ZDDP lubrication. ZDDP tribofilms can prevent direct contact of the rubbing surfaces and suppress the further graphitization of DLC coatings during rubbing. Overall, doping Ti with low content (0.7–5.8 at%) had a positive effect on friction and wear reduction of DLC/steel contact under boundary lubrication and facilitated the formation of continuous ZDDP tribofilms.

Acknowledgment

This work was supported by the Pre-Research Program in National 13th Five-Year Plan (61409230603); Beijing Municipal Natural Science Foundation (3182032); Joint Fund of Ministry of Education for Pre-research of Equipment for Young Personnel Project (6141A02033120); the Tribology Science Fund of State Key Laboratory of Tribology (SKLTKF19B12); and Fundamental Research Funds for the Central University (2652019069 and 2652019224).

Conflict of Interest

There are no conflicts of interest.

Data Availability Statement

The datasets generated and supporting the findings of this article are obtainable from the corresponding author upon reasonable request. The authors attest that all data for this study are included in the paper. No data, models, or codes were generated or used for this paper.

References

- [1] Bewilogua, K., and Hofmann, D., 2014, "History of Diamond-Like Carbon Films—From First Experiments to Worldwide Applications," *Surf. Coat. Technol.*, **242**, pp. 214–225.
- [2] Matthews, A., and Eskildsen, S. S., 1994, "Engineering Applications of Diamond-Like Carbon," *Diamond Relat. Mater.*, **3**(4–6), pp. 902–911.
- [3] Kalin, M., Velkavrh, I., Vižintin, J., and Özbolt, L., 2008, "Review of Boundary Lubrication Mechanisms of DLC Coatings Used in Mechanical Applications," *Meccanica*, **43**(6), pp. 623–637.
- [4] Al Mahmud, K. A. H., Kalam, M. A., Masjuki, H. H., Mobarak, H. M., and Zulkifli, N. W. M., 2015, "An Updated Overview of Diamond-Like Carbon Coating in Tribology," *Crit. Rev. Solid State Mater. Sci.*, **40**(2), pp. 90–118.
- [5] Robertson, J., 2002, "Diamond-Like Amorphous Carbon," *Mater. Sci. Eng. R Rep.*, **37**(4–6), pp. 129–281.
- [6] Zhang, S. D., Yan, M. F., Yang, Y., Zhang, Y. X., Yan, F. Y., and Li, H. T., 2019, "Excellent Mechanical, Tribological and Anti-Corrosive Performance of Novel Ti-DLC Nanocomposite Thin Films Prepared Via Magnetron Sputtering Method," *Carbon*, **151**, pp. 136–147.
- [7] Yue, W., Liu, C. Y., Fu, Z. Q., Wang, C. B., Huang, H. P., and Liu, J. J., 2015, "Effects of Tungsten Doping Contents on Tribological Behaviors of Tungsten-Doped Diamond-Like Carbon Coatings Lubricated by MoDTC," *Tribol. Lett.*, **58**(2), p. 31.
- [8] Zhang, S. J., Yue, W., Kang, J. J., Wang, Y. Y., Fu, Z. Q., Zhu, L. N., She, D. S., and Wang, C. B., 2019, "Ti Content on the Tribological Properties of W/Ti-Doped Diamond-Like Carbon Film Lubricating With Additives," *Wear*, **430–431**, pp. 137–144.
- [9] Keuneecke, M., Bewilogua, K., Becker, J., Gies, A., and Grischke, M., 2012, "Cr/Ca-C:H Coatings for Highly Loaded, Low Friction Applications Under Formulated Oil Lubrication," *Surf. Coat. Technol.*, **207**, pp. 270–278.
- [10] De Barros Bouchet, M. I., Martin, J. M., Le-Mogne, T., and Vacher, B., 2005, "Boundary Lubrication Mechanisms of Carbon Coatings by MoDTC and ZDDP Additives," *Tribol. Int.*, **38**(3), pp. 257–264.
- [11] Gayathri, S., Kumar, N., Krishnan, R., Ravindran, T. R., Amirthapandian, S., Dash, S., Tyagi, A. K., and Sridharan, M., 2015, "Influence of Transition Metal Doping on the Tribological Properties of Pulsed Laser Deposited DLC Films," *Ceram. Int.*, **41**(1), pp. 1797–1805.
- [12] Tsai, P. C., Hwang, Y. F., Chiang, J. Y., and Chen, W. J., 2008, "The Effects of Deposition Parameters on the Structure and Properties of Titanium-Containing DLC Films Synthesized by Cathodic Arc Plasma Evaporation," *Surf. Coat. Technol.*, **202**(22–23), pp. 5350–5355.
- [13] Zhao, F., Li, H. X., Ji, L., Wang, Y. J., Zhou, H. D., and Chen, J. M., 2010, "Ti-DLC Films with Superior Friction Performance," *Diamond Relat. Mater.*, **19**(4), pp. 342–349.
- [14] Kalin, M., and Vižintin, J., 2006, "Differences in the Tribological Mechanisms When Using Non-Doped, Metal Doped (Ti, WC), and Non-Metal-Doped (Si) Diamond-Like Carbon Against Steel Under Boundary Lubrication, With and Without Oil Additives," *Thin Solid Films*, **515**(4), pp. 2734–2747.
- [15] Cui, J. F., Li, Q., Zhang, B., Xiao, L., Yang, T., and Zhang, J. Y., 2012, "Mechanical and Tribological Properties of Ti-DLC Films With Different Ti Content by Magnetron Sputtering Technique," *Appl. Surf. Sci.*, **258**(12), pp. 5025–5030.
- [16] Ma, G. J., Gong, S. L., Lin, G. Q., Zhang, L., and Sun, G., 2012, "A Study of Structure and Properties of Ti-Doped DLC Film by Reactive Magnetron Sputtering With Ion Implantation," *Appl. Surf. Sci.*, **258**(7), pp. 3045–3050.
- [17] Dai, W., Ke, P. L., Moon, M. W., Lee, K. R., and Wang, A., 2012, "Investigation of the Microstructure, Mechanical Properties and Tribological Behaviors of Ti-Containing Diamond-Like Carbon Films Fabricated by a Hybrid Ion Beam Method," *Thin Solid Films*, **520**(19), pp. 6057–6063.
- [18] Wang, Q. Z., Zhou, F., Zhou, Z. F., Yang, Y., Yan, C., Wang, C. D., Zhang, L. K., Li, Y., Bello, I., and Lee, S. T., 2012, "Influence of Ti Content on the Structure and Tribological Properties of Ti-DLC Coatings in Water Lubrication," *Diamond Relat. Mater.*, **25**, pp. 163–175.
- [19] Qiang, L., Gao, K. X., Zhang, L. F., Wang, J., Zhang, B., and Zhang, J. Y., 2015, "Further Improving the Mechanical and Tribological Properties of Low Content Ti Doped DLC Film by W Incorporating," *Appl. Surf. Sci.*, **353**, pp. 522–529.
- [20] Dhandapani, V. S., Subbiah, R., Thangavel, E., Arumugam, M., Park, K., Gasem, Z. M., Veeraragavan, V., and Kim, D. E., 2016, "Tribological Properties, Corrosion Resistance and Biocompatibility of Magnetron Sputtered Titanium-Amorphous Carbon Coatings," *Appl. Surf. Sci.*, **371**, pp. 262–274.
- [21] Zhou, S. G., Liu, L., Ma, L. Q., Wang, Y. C., and Liu, Z. B., 2017, "Influence of CH₄ Flow Rate on Microstructure and Properties of Ti-C:H Films Deposited by DC Reactive Magnetron Sputtering," *Tribol. Trans.*, **60**(5), pp. 852–860.
- [22] Mao, Y. M., Piliptsova, D. G., Rudenkov, A. S., Rogachev, A. V., Jiang, X. H., Sun, D. P., Chaus, A. S., and Balmakou, A., 2017, "Structure, Mechanical and Tribological Properties of Ti-Doped Amorphous Carbon Films Simultaneously Deposited by Magnetron Sputtering and Pulse Cathodic Arc," *Diam. Relat. Mater.*, **77**, pp. 1–9.
- [23] Guo, Y. Z., Guo, P., Sun, L. L., Li, X. W., Ke, P. L., Li, Q., and Wang, A. Y., 2019, "Tribological Properties of Ti-Doped Diamond-Like Carbon Coatings Under Dry Friction and PAO oil Lubrication," *Surf. Interface Anal.*, **51**(3), pp. 361–370.
- [24] Dhandapani, V. S., Kang, K. M., Seo, K. J., Kim, C. L., and Kim, D. E., 2019, "Enhancement of Tribological Properties of DLC by Incorporation of Amorphous Titanium Using Magnetron Sputtering Process," *Ceram. Int.*, **45**(9), pp. 11971–11981.
- [25] Vengudusamy, B., Green, J. H., Lamb, G. D., and Spikes, H. A., 2011, "Tribological Properties of Tribofilms Formed From ZDDP in DLC/DLC and DLC/Steel Contacts," *Tribol. Int.*, **44**(2), pp. 165–174.
- [26] Yue, W., Liu, C. Y., Fu, Z. Q., Wang, C. B., Huang, H. P., and Liu, J. J., 2014, "Effects of Molybdenum Dithiocarbamate and Zinc Dialkyl Dithiophosphate

- Additives on Tribological Behaviors of Hydrogenated Diamond-Like Carbon Coatings," *Mater. Des.*, **64**, pp. 601–607.
- [27] Yang, L. Q., Neville, A., Brown, A., Ransom, P., and Morina, A., 2014, "Friction Reduction Mechanisms in Boundary Lubricated W-Doped DLC Coatings," *Tribol. Int.*, **70**, pp. 26–33.
- [28] Ciarsolo, I., Fernández, X., de Gopegui, U. R., Zubizarreta, C., Abad, M. D., Mariscal, A., Caretti, I., Jiménez, I., and Sánchez-López, J. C., 2014, "Tribological Comparison of Different C-Based Coatings in Lubricated and Unlubricated Conditions," *Surf. Coat. Technol.*, **257**, pp. 278–285.
- [29] Kosariéh, S., Morina, A., Lainé, E., Flemming, J., and Neville, A., 2013, "Tribological Performance and Tribochemical Processes in a DLC/Steel System When Lubricated in a Fully Formulated Oil and Base Oil," *Surf. Coat. Technol.*, **217**, pp. 1–12.
- [30] Dorgham, A., Parsaeian, P., Neville, A., Ignatyev, K., Mosselmans, F., Masuko, M., and Morina, A., 2018, "In Situ Synchrotron XAS Study of the Decomposition Kinetics of ZDDP Triboreactive Interfaces," *RSC Adv.*, **8**(59), pp. 34168–34181.
- [31] Kalin, M., Roman, E., Özbolt, L., and Vižintin, J., 2010, "Metal-Doped (Ti, WC) Diamond-Like Carbon Coatings: Reactions With Extreme-Pressure Oil Additives Under Tribological and Static Conditions," *Thin Solid Films*, **518**(15), pp. 4336–4344.
- [32] Spikes, H., 2004, "The History and Mechanisms of ZDDP," *Tribol. Lett.*, **17**(3), pp. 469–489.
- [33] Wang, Y. Y., Yue, W., She, D. S., Fu, Z. Q., Huang, H. P., and Liu, J. J., 2014, "Effects of Surface Nanocrystallization on Tribological Properties of 316L Stainless Steel Under MoDTC/ZDDP Lubrications," *Tribol. Int.*, **79**, pp. 42–51.
- [34] Ferrari, A. C., and Robertson, J., 2000, "Interpretation of Raman Spectra of Disordered and Amorphous Carbon," *Phys. Rev. B*, **61**(20), pp. 14095–14107.
- [35] Ferrari, A. C., and Robertson, J., 2001, "Resonant Raman Spectroscopy of Disordered, Amorphous, and Diamondlike Carbon," *Phys. Rev. B*, **64**(7), p. 075414.
- [36] Okubo, H., and Sasaki, S., 2017, "In Situ Raman Observation of Structural Transformation of Diamond-Like Carbon Films Lubricated With MoDTC Solution: Mechanism of Wear Acceleration of DLC Films Lubricated With MoDTC Solution," *Tribol. Int.*, **113**, pp. 399–410.
- [37] Jo, Y. J., Zhang, T. F., Son, M. J., and Kim, K. H., 2018, "Synthesis and Electrochemical Properties of Ti-Doped DLC Films by a Hybrid PVD/PECVD Process," *Appl. Surf. Sci.*, **433**, pp. 1184–1191.
- [38] <https://srdata.nist.gov>.
- [39] Wagner, C. D., Riggs, W. M., Davis, L. E., and Moulder, J. F., 1979, *Handbook of X-ray Photoelectron Spectroscopy*, Perkin-Elmer Corp., Physical Electronics Division, USA.
- [40] Meng, W. J., Tittsworth, R. C., and Rehn, L. E., 2000, "Mechanical Properties and Microstructure of TiC/Amorphous Hydrocarbon Nanocomposite Coatings," *Thin Solid Films*, **377–378**, pp. 222–232.
- [41] Musil, J., Kunc, F., Zeman, H., and Polakova, H., 2002, "Relationships Between Hardness, Young's Modulus and Elastic Recovery in Hard Nanocomposite Coatings," *Surf. Coating Technol.*, **154**(2–3), pp. 304–313.
- [42] Lin, Y. H., Lin, H. D., Liu, C. K., Huang, M. W., Chen, J. R., and Shih, H. C., 2010, "Structure and Characterization of the Multilayered Ti-DLC Films by FCVA," *Diamond Relat. Mater.*, **19**(7–9), pp. 1034–1039.
- [43] Vengudusamy, B., Green, J. H., Lamb, G. D., and Spikes, H. A., 2013, "Influence of Hydrogen and Tungsten Concentration on the Tribological Properties of DLC/DLC Contacts with ZDDP," *Wear*, **298–299**, pp. 109–119.
- [44] Liu, Y., and Meletis, E. I., 1997, "Evidence of Graphitization of Diamond-Like Carbon Films During Sliding Wear," *J. Mater. Sci.*, **32**(13), pp. 3491–3495.
- [45] Cheng, Y. C., Jin, C. Q., Gao, F., Wu, X. L., Zhong, W., Li, S. H., and Chu, P. K., 2009, "Raman Scattering Study of Zinc Blende and Wurtzite ZnS," *J. Appl. Phys.*, **106**(12), p. 123505.
- [46] Berkani, S., Dassenoy, F., Minfray, C., Martin, J. M., Cardon, H., Montagnac, G., and Reynard, B., 2013, "Structural Changes in Tribo-Stressed Zincpolyphosphates," *Tribol. Lett.*, **51**(3), pp. 489–498.
- [47] Xu, D. C., Wang, C., Espejo, C., Wang, J. G., Neville, A., and Morina, A., 2018, "Understanding the Friction Reduction Mechanism Based on Molybdenum Disulfide Tribofilm Formation and Removal," *Langmuir*, **34**(45), pp. 13523–13533.
- [48] Ren, S. M., Zheng, S. X., Pu, J. B., Lu, Z. B., and Zhang, G. A., 2015, "Study of Tribological Mechanisms of Carbon-Based Coatings in Antiwear Additive Containing Lubricants Under High Temperature," *RSC Adv.*, **5**(81), p. 66426–66437.
- [49] Crobu, M., Rossi, A., Mangolini, F., and Spencer, N. D., 2010, "Tribochemistry of Bulk Zinc Metaphosphate Glasses," *Tribol. Lett.*, **39**(2), pp. 121–134.
- [50] Dorgham, A., Azam, A., Morina, A., and Neville, A., 2018, "On the Transient Decomposition and Reaction Kinetics of Zinc Dialkylthiophosphate," *ACS Appl. Mater. Interfaces*, **10**(51), pp. 44803–44814.
- [51] Parsaeian, P., Van Eijk, M. C. P., Nedelcu, I., Neville, A., and Morina, A., 2017, "Study of the Interfacial Mechanism of ZDDP Tribofilm in Humid Environment and Its Effect on Tribochemical Wear; Part I: Experimental," *Tribol. Int.*, **107**, pp. 135–143.
- [52] Parsaeian, P., Ghanbarzadeh, A., Van Eijk, M. C. P., Nedelcu, I., Neville, A., and Morina, A., 2017, "A New Insight Into the Interfacial Mechanisms of the Tribofilm Formed by Zinc Dialkyl Dithiophosphate," *Appl. Surf. Sci.*, **403**, pp. 472–486.